The 2015 World Congress on
Advances in Civil, Environmental, and Materials Research (ACEM15)
Incheon, Korea, August 25-29, 2015

A modified boundary treatment in the Incompressible SPH for accurate pressure calculation on the solid boundary

*Nur`Ain Idris[1)] , Mitsuteru Asai[2)] and Yoshimi Sonoda[3)]

[1), 2), 3)] *Department of Civil Engineering, Kyushu University, 744 Motooka, Nishi-ku, Fukuoka 819-0395, Japan*
[1)] nurain@doc.kyushu-u.ac.jp

ABSTRACT

The Incompressible Smoothed Particle Hydrodynamic (ISPH) is one of the particle methods and commonly used to solve some complicated physical problems including free surface flow problems. The study regarding the boundary treatment has become an active research area in the mesh-free or particle method recently for measuring the accurate and robust pressure near the boundary. The penetrations of fluid particles may be happened if the adequate pressure boundary condition on the solid boundary cannot be satisfied. In this paper, a simple boundary treatment, which can be satisfied the non-homogenous Neumann boundary condition on the solid boundary and Dirichlet condition on the water surface, is proposed. The key point of our proposed treatment is that these boundary conditions are automatically satisfied by solving a modified pressure Poisson equation. Although the application of a similar ideas proposed by Mayrhofer (2014) is limited to a simple solid boundary shape, our technique can be applied to arbitrary shape with concave-convex boundary. Lastly, the effectiveness and accuracy of boundary treatment proposed are then authenticated with couples of numerical analysis and compared with the experimental tests.

1. INTRODUCTION

Smoothed particle hydrodynamics (SPH) is a Lagrangian meshless particle method that has been popular and actively used by researchers especially in computational fluid dynamics nowadays. This SPH method was first developed by Lucy(1977) and Gingold(1977) which originated from simulation of the astrophysical problems about

---

[1)] Graduate Student
[2)] Associate Professor
[3)] Professor

three decades ago. SPH method is a unique particle method which does not required any grid and has some advantages over grid based method such as simple in implementation and also eases of handling even for complex fluid and larger deformations. Then, the SPH method was extended to incompressible viscous flow (Monaghan 1994). Nowadays, a stabilized Incompressible Smoothed Particle Hydrodynamic (ISPH) approach is one of the particle methods and commonly used to solve some of complicated physical problems including free surface flow problems (Asai 2012). In addition, boundary treatment of the particle method is one of the important issue for accurate solutions. Many researchers tried to improving the boundary treatment from the ghost particle by Yildiz(2009) then fixed ghost particle by Marrone(2011), and virtual marker by Asai(2013) and until know this research topic still become an vigorous research area. Therefore, in this a modified boundary treatment is presented, which resolves the problem of pressure accuracy near the boundary including the prevention the penetration.

2. A STABILIZED INCOMPRESSIBLE SMOOTHED PARTICLE HYDRODYNAMICS (ISPH)

In this paper, the basic of stabilized ISPH which introduced by Asai (2012) was adopted. The concept of ISPH was including the modification of source term in the treatment of pressure Poisson equation (PPE). In the following sections, will be described the governing equations used and the concept of Smoothed Particle Hydrodynamics (SPH) with the modification for incompressible flow.

2.1 Governing equation

The continuity equation and the Navier- Stokes equation in the Lagrange description are given as follows;

$$\frac{D\rho}{Dt} + \rho\nabla\cdot\mathbf{u} = \mathbf{0} \tag{1}$$

$$\frac{D\mathbf{u}}{Dt} = -\frac{1}{\rho}\nabla p + \nu\nabla^2\mathbf{u} + \frac{1}{\rho}\nabla\cdot\boldsymbol{\tau} + \mathbf{F} = \mathbf{0} \tag{2}$$

where ρ and ν are density and kinematic viscosity of fluid, **u** and *p* are the velocity vector and pressure of fluid respectively. **F** is an external force, and *t* indicates time. The turbulence stress $\boldsymbol{\tau}$ is necessary to represent the effects of the turbulence with coarse spatial grids. In the most general incompressible flow approach, the density is assumed by a constant value with its initial value. Then the above mentioned governing equations lead to

$$\nabla \cdot \mathbf{u} = \mathbf{0} \tag{3}$$

$$\frac{D\mathbf{u}}{Dt} = -\frac{1}{\rho^0}\nabla p + \nu\nabla^2\mathbf{u} + \frac{1}{\rho^0}\nabla \cdot \boldsymbol{\tau} + \mathbf{F} = \mathbf{0} \tag{4}$$

2.2 Smoothed Particle Hydrodynamics (SPH) Approach

The fundamental of SPH is based on the interpolation method. The interpolation is based on the theory of integral interpolants by using kernels which approximate a delta function. A function $\phi(x_i, t)$ at sampling point x_i can be expressed in integral form as follow:

$$\phi(x_i, t) = \int W(x_i - x_j, h)\phi(x_j, t)dv = \int W(r_{ij}, h)\phi(x_j, t)dv \tag{5}$$

where *W* is a weight function called as a smoothing kernel function and the subscript *i* and *j* indicate the positions of labeled particle. In the smoothing kernel function, $r_{ij} = |x_i - x_j|$ and *h* are the distance between neighbor particles and the smoothing length, respectively. The cubic spline function is used as a kernel function in this paper. For the SPH numerical analysis, the integral equation (5) is approximated by a summation of contributions from neighbor particles in the support domain as written:

$$\phi(r_i) \approx \langle \phi_i \rangle = \sum_j \frac{m_j}{\rho_j}\phi_j W(r_{ij}, h) \tag{6}$$

2.3 Stabilization of pressure in PPE

Generally, in SPH approach, there some difficulty occurred due to the accuracy of the density representation in the SPH formulation and the treatment of pressure Poisson

equation (PPE). It is difficult for the numerical densityto keep its initial value. Therefore, here, the PPE is reconsidered to overcome the error of artificial pressure fluctuation in the ISPH. In density invariance scheme, the particle position updates after each predictor step and the particle density is updated on the intermediate particle positions. While in the correction step, the pressure term is used to update the particle velocity obtained from the intermediate step. Then, the final form of PPE in ISPH can be approximately redefined by

$$< \nabla^2 p_i^{n+1} > = \frac{\rho^0 - \langle \rho_i \rangle}{\Delta t^2} \tag{7}$$

Instead of the projection schemes in ISPH as mentioned afore, Asai et al. (2012) was proposed an efficient and robust ISPH scheme which using both conditions without internal iteration as stabilizing method for the ISPH. The modification is made without additional calculations, except for the source term in PPE which slightly changed from the original ISPH as follows:

$$< \nabla^2 p_i^{n+1} > = \frac{\rho^0}{\Delta t} < \nabla \cdot \mathbf{u}_i^* > + \alpha \frac{\rho^0 - < \rho_i^n >}{\Delta t^2} \tag{8}$$

Whereby they are introducing the relaxation coefficient, α ($0 \leq \alpha \leq 1$) and usually the small value is used around 1% or less. In this study, the stabilized ISPH with the turbulent viscosity will be applied to.

3. BOUNDARY TREATMENT

3.1 Slip and non-slip condition with virtual marker

The virtual marker proposed to be located in a position which is symmetrical to the wall particle across it solid boundary whereas the wall particles is placed on a grid like structure. There are a few procedures on how slip or non-slip condition of virtual marker as the boundary treatment that will be describe later. Normally, the velocity and pressure on the marker are interpolated based on the concept of weighted average of neighboring particles, which is the fundamental equation of SPH as in the Eq. (6). However, the portion of the particles within the compact support might be in the wall domain or unoccupied domain such as air phase. For that case, the interpolation

approximation will used the modified weight function ($\tilde{W}$) as shown below.

$$\phi(\boldsymbol{x}_i,t) \approx \langle \phi_i \rangle = \sum_j \frac{m_j}{\rho_j} \tilde{W}(r_{ij},h) \phi_j(\boldsymbol{x}_j,t) \tag{9}$$

Where,

$$\tilde{W} = \frac{W(r_{ij},h)}{\sum_j \frac{m_j}{\rho_j} W(r_{ij},h)} \tag{10}$$

Note that, the key point here is the virtual marker is not directly associated with the SPH approximation but only a computational point to give the wall particle accurate physical properties. Therefore, the density of the virtual marker does not have a bad influence on accuracies in SPH and hence, there is high possibility to make the boundary condition more robustly. Then, the velocity on the virtual marker which is corresponding to the wall particle across its solid boundary is interpolated by the SPH approximation. As mentioned earlier, there are several conditions such as slip condition, non-slip condition or mixed condition. In order to satisfy the slip condition, the wall particle required to be given the velocity, which is mirror-symmetric to the one on the virtual marker. This mirroring processing is given by the following equation.

$$\boldsymbol{v}_w' = \boldsymbol{M}\boldsymbol{v}_v \quad , \quad M_{ij} = \delta_{ij} - 2n_i n_j \tag{11}$$

Where ***M*** is a second order tensor to implement the mirroring processing, and it is symbolized by using inward normal vector of the wall and the kronecker delta. On the other hand, in order to satisfy the non-slip condition, the wall particle needs to be given the velocity, which is point-symmetrical to the virtual marker as shown in Eq. (12) whereas ***R*** is a mirror symmetric tensor.

$$\mathbf{v}_w' = \mathbf{R}\mathbf{v}_v \quad , \quad R_{ij} = -\delta_{ij} \tag{12}$$

Practically, it is necessary to discuss an optimized condition between slip and no-slip condition to refer the resolution of the simulation model. Therefore, the following equation is proposed by using the coefficient of β ($0 \leqq \beta \leqq 1$) which can be consider as mixed condition.

$$\mathbf{v}_w' = \beta\mathbf{M}\mathbf{v}_v + (1-\beta)\mathbf{R}\mathbf{v}_v \quad (0 \le \beta \le 1) \tag{13}$$

where β represents the ratio between slip and no-slip condition. In order to prevent from penetration of the water particle into the solid boundary, the pressure Neumann condition needs to be satisfied. For this purpose, giving the accurate pressure to the wall particle is necessary by referring to the one on the marker. Since normal component of the velocity on the solid boundary needs to be zero, the following equation needs to be satisfied.

$$\mathbf{v}_{w0} \cdot n = 0 \tag{14}$$

3.2 Pseudo Neumann boundary condition : Dirichlet conditions

Using the similar approach as introduced by Asai (2013), the pressure on each virtual marker and the external force will evaluated by using the physical quantity in the particles neighborhood as in (9) with the normalized weight function in (10). Thus, the pressure on the walls particles in the border processing technique does not directly evaluated by solving the modified pressure Poisson equation (8). By introduced solving the PPE will gave entire circumference of Dirichlet condition whereby approximation of the value of the wall particles pressure by referring the value of the virtual marker as to satisfy the Neumann boundary condition. Note that, a Dirichlet boundary will give the zero pressure of the particles of the free surface as customary. This means that this method is not strictly satisfy the pressure of Neumann boundary conditions. In addition, since the coefficient matrix of the Poisson equation remains symmetric matrix need not be modified, the solver of the simultaneous linear equations conjugate gradient method using a diagonal scaling pre-processing (CG) method was used.

3.3 Neumann boundary treatment (completely satisfy the pressure Neumann conditions)

In this section, the Modified Virtual Marker with Regular grid (MVMRG) as new boundary treatment which satisfied the non-homogenous Neumann boundary condition will be describe The concept of this treatment is to give a wall particle accurate physical properties, velocity and pressure. As concern, the virtual marker used in the previous section, which is a pseudo Neumann condition is convenient to perform the analysis including the rate of real condition as slip or non-slip condition. However, by solving PPE with the giving the entire circumference Dirichlet condition of zero pressure causes a

lower pressure value than the actual hydrostatic pressure distribution in the vicinity of wall particles. Therefore, the MVMRG is proposed in order to overcome this problem and at once attempt to strictly satisfying the non-homogenous Neumann boundary conditions.

The procedures will be described briefly. First, the wall particles placing similarly as in Pseudo Neumann condition method which placed equally spaced structural grid-like inside solid. Then, the location of the virtual markers are located on the boundary surface which now no longer in the fluid domain. Therefore, by placing the wall particles on structured grid, the position X' of the virtual markers in the method uses the distance d to the normal vector n and the boundary on the actual physical interface become as follows

$$\boldsymbol{X}' = \boldsymbol{X} + d\boldsymbol{n} \tag{15}$$

The process of calculated the value of the inner speed on the virtual marker is similar with the previous section which using the SPH approximation as in Eq. (9) and also the flow rate of physical quantity either slip condition or non-slip condition or mixed condition as from Eq. (11) to (13). However, because in the border processing techniques are disposed on the entire virtual markers interface, given the flow velocity is not strictly mirror-symmetrical or point-symmetrical. Therefore, the modification of the coefficient matrix and the source term to meet the pressure Neumann condition need to be conducted. Therefore, pressure Dirichlet conditions at the stage of solving the Poisson equation was applied only to the place given originally, and at the same time propose method to simultaneously satisfy the pressure Neumann conditions. At the first place, the pressure Neumann boundary condition need to be satisfied on the boundary surface as well as in Pseudo Neumann condition discussed previously. Furthermore, in order to satisfy the non-homogenous Neumann boundary condition, some medication was made and the pressure approximation of wall particles is evaluated by using the following equation.

$$P'_{\mathrm{w}} = P_{\mathrm{w0}} + d\rho\, \boldsymbol{f}_{\mathrm{w0}} \cdot \boldsymbol{n} \tag{16}$$

From now, the pressure and the external force in the *w0* points are projected from the teeth or on the boundary surface. Note that, this *w0* point is generally not arranged

particles, it is necessary to approximate the value of the particle around in some way. Therefore, by using the MVMRG, the value of the water particles around w0 referred can be approximated as follows.

$$P_{\mathrm{w}0} \cong \overline{P}_{\mathrm{v}} = \frac{\sum_{j \in water}^{n_w} P_j}{n_w}; \quad \boldsymbol{f}_{\mathrm{w}0} \cong \bar{\boldsymbol{f}}_{\mathrm{v}} = \frac{\sum_{j \in water}^{n_w} \boldsymbol{f}_j}{n_w} \tag{17}$$

By using this approximation, then the Eq. (35) can be approximately defined by the following equation.

$$P'_{\mathrm{w}} = \overline{P}_{\mathrm{v}} + d\rho\, \bar{\boldsymbol{f}}_{\mathrm{v}} \cdot \boldsymbol{n} \tag{18}$$

Although the above equation looks similar to the Pseudo condition, but differences exists in the right-hand terms due to the placement of virtual marker on the boundary surface. Even it is a simple averaging of the neighboring particles, the pressure of the number of water particles present in the influence radius has been concentrated on the virtual markers and will evaluate by using an external force. Therefore, the treatment for calculated the pressure in the SPH formulation will be a bit different.

As shown in Eq. (17), it is intended to give the relationship between the pressure on the water particles which near to the unknown pressure of the wall particles. Therefore, by using the above techniques, the pressure solved by the PPE can be limited to the water particles. Moreover, the special modification of the coefficient matrix and source terms when the particles discretized will also discussed. Then, it will become as below.

$$m_{\mathrm{w}} \left(\frac{\rho_i + \rho_{\mathrm{w}}}{\rho_i \rho_{\mathrm{w}}} \frac{\mathbf{r}_{i\mathrm{w}} \cdot \nabla W\left(r_{i\mathrm{w}}, h\right)}{\mathbf{r}_{i\mathrm{w}}^2 + \eta^2} \right) \left(P_i - P'_{\mathrm{w}}\right) \tag{19}$$

Make it in more simplify way, the related coefficients as follows

$$A_{i\mathrm{w}} \left(P_i - P'_{\mathrm{w}}\right) \tag{20}$$

On the other hand, the substitution of Eq. (17) into Eq. (20), and also substituting the Eq. (18) shows as follows.

$$A_{iw}\left\{P_i-\left(\overline{P}_v+d\rho\,\bar{\boldsymbol{f}}_v\cdot\boldsymbol{n}\right)\right\}$$

$$A_{iw}\left\{P_i-\left(\frac{\sum_{j\in water}^{n_w}P_j}{n_w}+d\rho\frac{\sum_{j\in water}^{n_w}\boldsymbol{f}_j}{n_w}\cdot\boldsymbol{n}\right)\right\}$$

$$A_{iw}\left\{P_i-\frac{\sum_{j\in water}^{n_w}P_j}{n_w}-b_i\right\} \tag{21}$$

Noted that, the simplification is made from simple averaging of the external force and all components of the relevant coefficient matrix and source terms are rearranged in the water particles in the vicinity. By solving this Poisson equation coefficient matrix and the source term, it is automatically satisfied the non-homogeneous of pressure Neumann conditions. However, it should be noted that the coefficient matrix has been modified and become an asymmetrical matrix and the solver of simultaneous linear equations adopted was Bi-CGSTAB method. In such a proposed method, a factor produced between the wall particles and water particles, which are converted to water particles in the vicinity of the wall particles. The relationship which the concept mentioned above between the virtual marker, water particles and the wall particles as shown in Fig. 1.

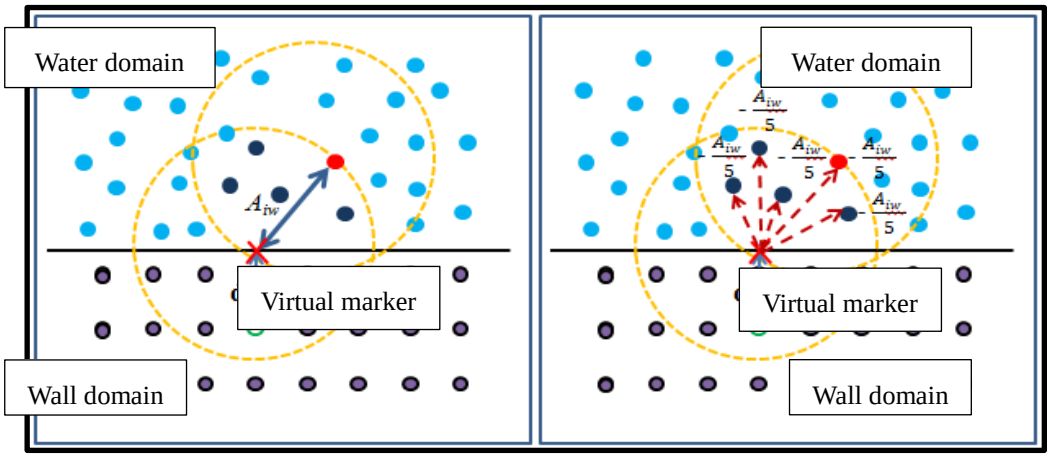

Fig. 1 The relationship of the modified virtual marker on the boundary with the wall particles and water particles

Note that, after solving the PPE abovementioned, the pressure need to go through mapping process which is the expression can be used for mapping step as follows. Whereas the pressure and the external force except for the virtual marker will be analyzed by SPH formulation as in Eq. (9) which, depending on the normalized weight function as in Eq. (10).

$$P'_{\mathrm{w}} = < P_{\mathrm{v}} > + d\rho < \boldsymbol{f}_{\mathrm{v}} > \cdot \boldsymbol{n} \tag{22}$$

The flow rate on the wall particles choose in this treatment is similarly with the flow rate condition discussed in the previous section. As described above, in solving a modified Poisson equation in the virtual marker method lead to natural ways which is non-homogenous is characterized as pressure field produced is satisfied the pressure Neumann condition. Moreover, the virtual marker position in this border led to processing technique created only once in the pre-process. However, the coefficient matrix in solving the pressure Poisson equation becomes asymmetric matrix, causes higher in the calculation load. There are some verification and validation test was made using this new modification which is used MVMRG to see the performance and also in comparison with experimental test that will be discussed in the following sections.

4. VERIFICATION AND VALIDATION

In this section, there are several numerical test were conducted in order to verify and validate the modified boundary treatment proposed, MVMRG in this paper. The first example test is a simple hydrostatic problem. There are 2 different condition of boundary surface for hydrostatic test whereas the simplest one with compatible boundary surface and compatible surface with arbitrary shape or more complex objects. Then, the application on the dam break problem with an opening gate is presented to examine its applicability and simulation demonstration for comparison with the real experiment test.

4.1 Verification with Hydrostatic test

The first test is the simplest hydrostatic problem which the rectangular tank with compatible surface and filling water inside. The comparison of the pressure distribution was made between different boundary treatments which are using previous boundary treatment, pseudo Neumann condition and proposed modified boundary treatment, MVMRG which is fully satisfied Neumann boundary condition. This test was conducted to show the robustness of our modified boundary treatment. The tank was filled up with the water volume of 0.2m x 0.2m x 0.2m and the particles size is 0.01m. The theoretical hydrostatic pressure is given by a law, $p=\rho gh$ (= 980N/m^2) with water density ρ = 1000kg/m^3 and the water height h = 0.2m. Where, the point of pressure measurement is located in the middle of bottom tank. Fig. 2 shows the different results on the contour pressure distribution especially the effects near the bottom of the tank which obtained using different treatment. It is clearly show that there are high pressure distribution using the proposed modified treatment, using MVMRG boundary treatment compared with the Pseudo Neumann boundary condition that give lower pressure distribution especially near the edge of boundary. Then, the numerical result of the hydrostatic pressure were used to compared with the theoretical of value of hydrostatic pressure as shown in Fig. 3. Obviously, the result obtained by using modified boundary treatment of Neumann condition, MVMRG gives almost similar result with the theoretical. However, the result found from Pseudo Neumann treatment gives the lower value especially near the bottom surface due to the treatment used at the boundary surface not perfectly treat as non-homogenous of Neumann condition.

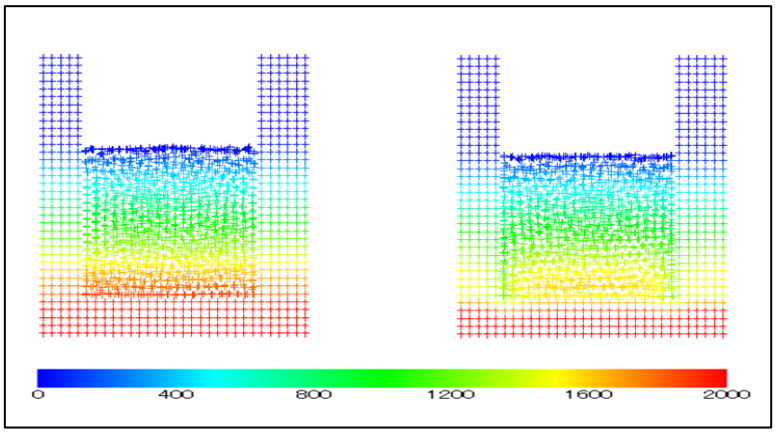

(a) (b)

Fig. 2 The pressure distribution on the water particles and wall boundary by (a) using MVMRG with perfectly Neumann condition and (b) Pseudo Neumann boundary condition for compatible surface boundary

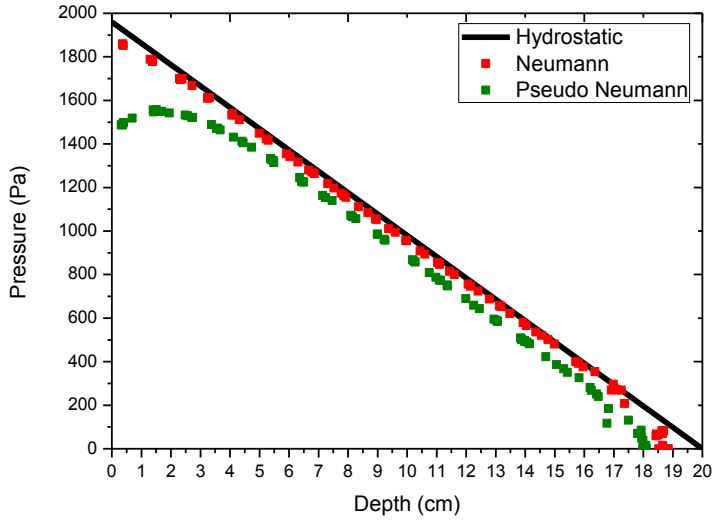

Fig. 3 The comparison of pressure distribution with the depth by using hydrostatic pressure, perfectly Neumann boundary treatment and Pseudo Neumann boundary condition for compatible surface boundary

Next, the same setup of water tank with the fill water but with the additional of several geometrical object or can considered as compatible surface with complex geometrical object submerged into the water. There are three complex shapes with concave-convex boundary have been chosen in this hydrostatic test such as the semi hemispheric shape, the pyramid shapes, and the concave with rectangular shapes as shown in the Fig. 4 (a) and (b). The height of the water level is same as the previous test which is 0.2m and the measurement point also located at the center of the bottom water tank. This time, the size of the particles is reduced to 0.005m which is higher resolution model compared to the previous case. Generally, Fig. 4 shows the pressure distribution inside the water domain and also the pressure distribution at the concave-convex shape boundary surface without any penetration occurred in both treatments. It can be seen, that by using the proposed boundary treatment, MVMRG gives higher pressure distribution for not only water domain but also to the arbitrary objects surface and there is no penetration occurred as depicted in Fig. 4 (c) and (d). Moreover, Fig. 4 (e) and (f) which is the view from the top shows the clear pressure gradient and also the pressure contour discrepancy by using different treatment of boundary condition.

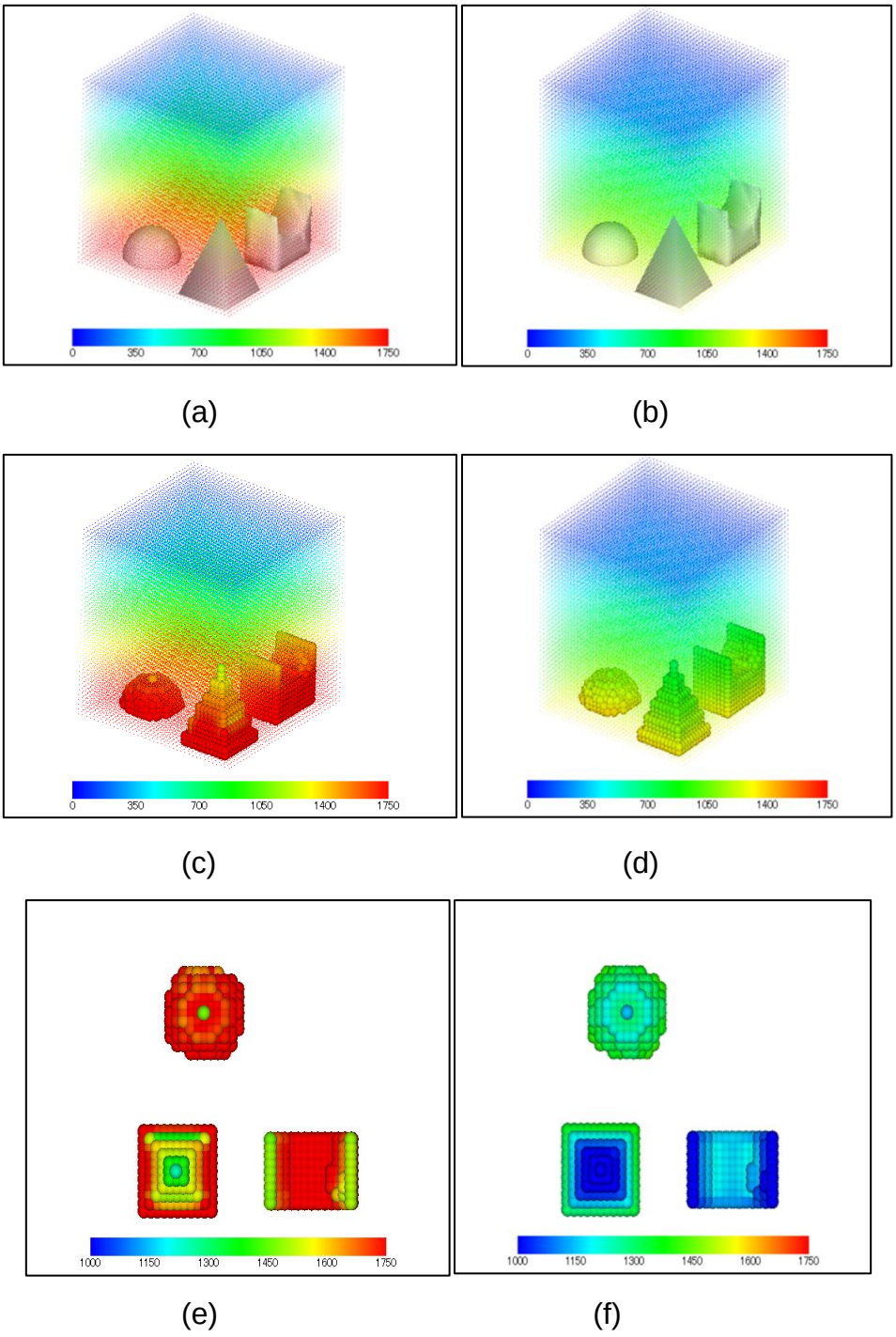

Fig. 4 The comparison of the pressure distribution using the modified boundary treatment which satisfied Neumann boundary condition with the treatment using Pseudo Neumann boundary condition: (a) the real shape of complex geometrical objects with pressure distribution of water using MVMRG with perfectly Neumann condition, (b) the

real shape of complex geometrical objects with pressure distribution of water using Pseudo Neumann condition, (c) pressure distribution of water particles and objects' surface using MVMRG with perfectly Neumann condition, (d) pressure distribution of water particles and objects' surface using Pseudo Neumann condition, (e) the pressure gradient of complex geometrical objects from the top view using MVMRG with perfectly Neumann condition, (f) the pressure gradient of complex geometrical objects from the top view using Pseudo Neumann condition.

Then, the numerical results of the pressure distribution were used for comparison purposed with the theoretical hydrostatic pressure as shown in Fig. 5. Based on the result obtained, the result using MVMRG with perfectly Neumann boundary condition gives higher value compared with the Pseudo Neumann condition that gives lower value especially near the boundary. Even though the pressure value still lower compared with the theoretical yet it shows an improvement of pressure distribution. The similar idea of using semi-analytical of wall boundary condition which led to satisfied the Neumann boundary condition by Mayrhofer (2014) also make a hydrostatic test for arbitrary shape without considering the more complicated shape as concave-convex shape and there is limitation of viscosity whereas the smallest viscosity may affect the accuracy of the result.

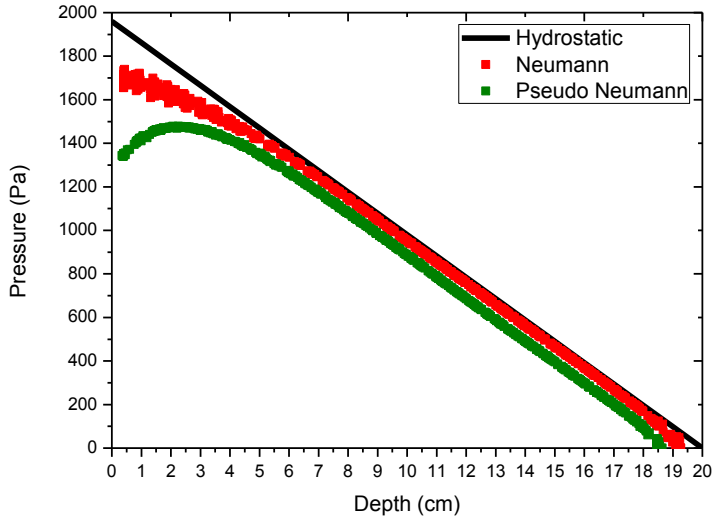

Fig. 5 The comparison of pressure distribution by using MVMRG with perfectly Neumann condition and Pseudo Neumann condition with the theoretical value hydrostatic pressure for compatible surface with complex geometrical objects

4.2 Validation with 3D Dam Break Flow with the Opening Gate

The simulation of three dimensional dam break flow is used to validate the versatility of our proposed method and compared with the experimental results. The experimental test on the investigation of dynamic pressure loads during dam break with an opening gate that was carried out at Technical University of Madrid (UPM) as reported by Lobovsky (2014) is used as the reference for simulate purposed. In order to validate the proposed modified boundary treatment with the experiment, the analysis model with the same geometry as the experimental including the five pressure sensors were used as shown in the schematic diagram (Fig. 6). In Fig. 6 (a), the front view and the top view of the analysis model shows the tank dimensions and the initial water depth H in the dam reservoir. The water depth and the velocity of the opening gate used for analysis model are 600mm and 4.53 m s^{-1} respectively. In addition, the water properties give the density of 997 kg m^{-3} and the kinematic viscosity of 8.9 x 10-7 m^2s^{-1}. While the arrangement of the pressure sensors used in the analysis model is illustrate as in the Fig. 6 (b). There are four sensors located in the center-line which the first sensor (sensor 1) is placed 3mm above the bed in order to measure the impact of pressure at the lower tank corner. While, the others three pressure sensors of the center-line are located at 15mm (sensor 2), 30mm (sensor 3), and 80 mm (sensor 4) between their centers and the tank bed as shown in the Figure 16 (b). The additional pressure sensor (sensor 2L) which is off-centered sensor is located at the same height as the second lowered sensor, sensor 2 but halfway towards the back wall.

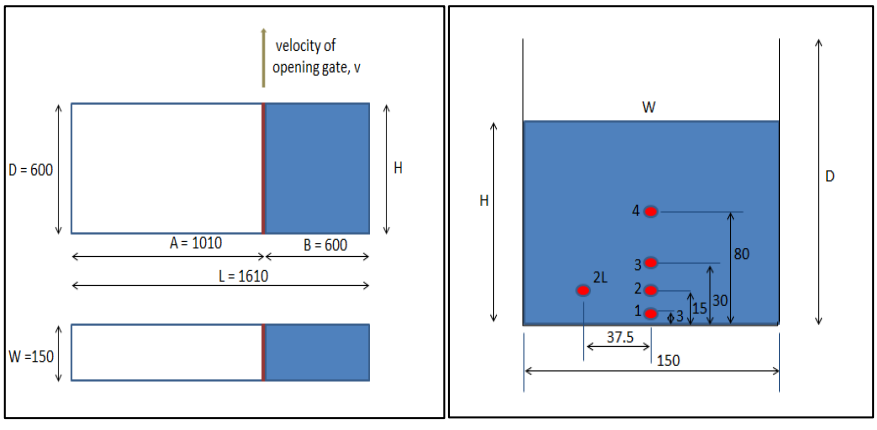

(a) (b)

Fig. 6 The dam break simulation with an opening gate which corresponding to the experiment conducted by Lobovsky (2014)

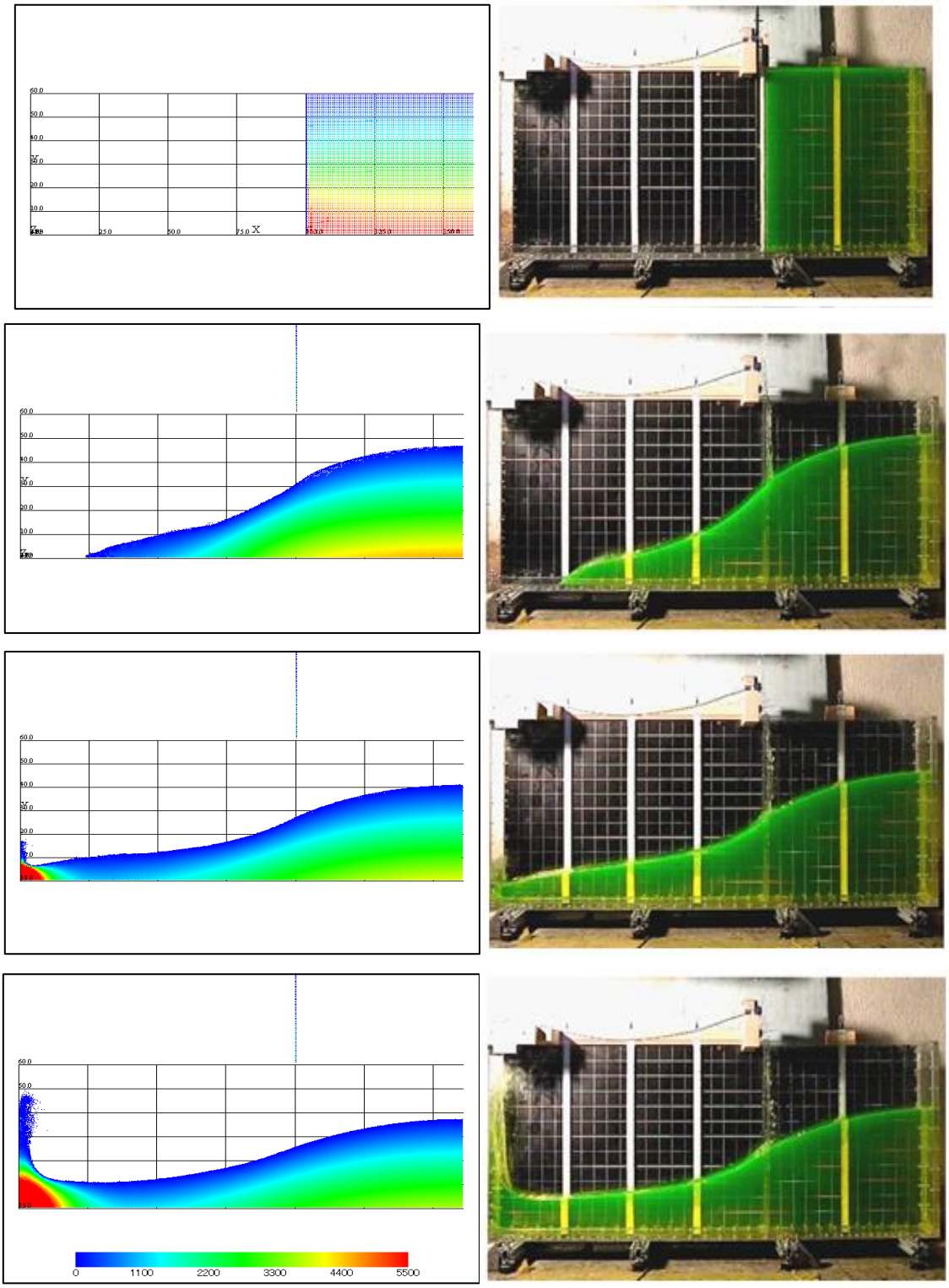

Fig. 7 The comparison of the free surface evolution between simulation and experimental at times 0.0, 316.7, 413.4, 463.3, and ±3.3ms

Fig. 7 shows the clear comparison of free surface profile evolution snapshot between the numerical simulation and the experimental at certain times. From the first observation, the effect of the dam gate removal looks similar at every snapshot on the free surface shape is observed. Then, the observation of the location of the wave front at each time of snapshot also shows the same tendency with the experiment. The pressure contour is also including in this figure which show the pressure gradient from the static condition before an opening gate and after gate's removal and the impact after hit the wall which shows higher pressure. Furthermore, from the snapshot, there is clear hint that the lowered sensors are exposed to the high pressure as the red color of contour is observed after the water smashed on the wall boundary surface. It is essentially, the impact pressure for each sensor is measured in order to compare with the results obtained from the experimental during the simulation.

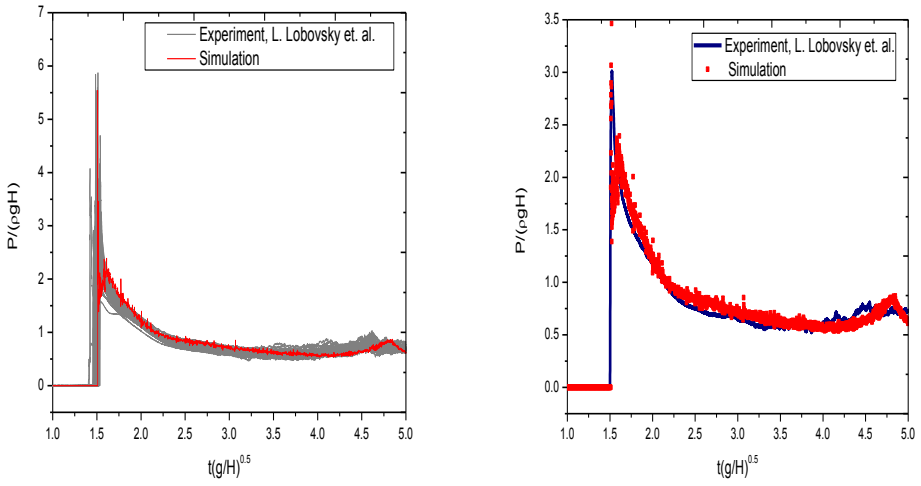

(a) (b)

Fig. 8 The comparison of the non-dimensional pressure with the non-dimensional time at sensor 1 (a) between the simulation results with the 100 test of experiment data (b) between the simulation results with the average pressure from the experimental

In Fig. 8, the results obtained at the lowered sensor (sensor 1) from the simulations are compared with the experimental data generally. Since, the experiment has been repeated for 100 times, and it is automatically produced some range of pressure data or

pressure time history analysis at sensor 1. Hence, the results obtained from the simulation for sensor 1 are used to compare with this 100 test of pressure time history as shown in Fig. 8 (a). It indicates the significant results, where the simulation results fall within the range of 100 tests of experimental results. Then, another comparison between typical impact event pressure signals from sensor 1 with the results obtained from simulation as shown in Fig. 8 (b). From the comparison, the arrival time from the numerical simulation is almost same with the arrival time in the experiment and also the tendency of the pressure time history is quite similar.

5. CONCLUSION

The numerical simulation that been conducted using the proposed boundary treatment, which using sing MVMRG with perfectly Neumann condition shows the good tendency and also more accurate pressure value near the boundary surface based on the hydrostatic tests and also the comparison with the experimental test for hydrodynamic pressure evaluation. The profile of the free surface also shows the similarity with result from the experiment. In addition, the comparison between Pseudo Neumann condition with the completely satisfied the Neumann boundary condition show clear discrepancy in the of pressure especially at the edge of bottom surface and this strongly proves that the proposed modified treatment which is perfectly non-homogenous Neumann condition gives the better treatment compared with Pseudo Neumann condition. As suggestion, more verification test can be conduct for the future works to ensure that the proposed boundary treatment is suitable for all cases.

REFERENCES

Asai, M. Aly, M.A. Sonoda, Y. and Sakai, Y. (2012) “A stabilized Incompressible SPH method by relaxing the density invariance condition” Journal of Applied Mathematics, Article ID 139583.

Asai, M. Fujimoto, K. Tanabe, S. and Beppu, M. (2013) “Slip and No-Slip Boundary Treatment for Particle Simulation Model with Incompatible Step-Shaped Boundaries by Using a Virtual Marker, Journal of JSCES, Paper No.20130011 (Japanese)

Gingold, R.A. and Monaghan, J.J. (1977) “Smoothed particle hydrodynamics: theory and application to non-spherical stars”, *Mon. Not. R. Astron Soc.*, Vol.181, pp. 375-389.

Lobovsky, L. Vera, E.B-. Castellana, F. Soler, J.M-. Iglesias, A.S-. (2014) “Experimental investigation of dynamic pressure loads during dam break”, Journal of Fluids and Structures 48 (2014) 407-434.

Lucy, L.B. (1977) “A numerical approach to the testing of the fusion process”, *Astron J.*, Vol.88, pp.1013-1024.

Marrone,S. Antuono,M. Colagrossi,A. . Colicchio, G. Touze, D.L. and Graziani,G. (2011) “δ-SPH model for simulating violent impact flows”, *Comput. Methods Appli. Mech. Engrg.*,Vol. 200, pp. 1526-1542,

Mayrhofer, A., Ferrand, M., Kassiotis, C., Violeau, D., and Morel, F.-X. (2014), “Unified semi-analytical wall boundary conditions in SPH: analytical extension to 3-D”, *Numer.Algorithms,* 68:15-34.

Monaghan, J.J. (1994) “Simulating Free Surface Flows with SPH”, Journal of Computational Physics, Vol. 110, pp.399-406,.

Yildiz, M. Rook, R. A. and Suleman, A. (2009) “SPH with the multiple boundary tangent method”, *Int. J. Numer. Meth. Engng.*, Vol. 77, pp. 1416-1438.